Photonics and Optoelectronics

A Polarization-Encoded Photon-to-Spin Interface

K. C. Chen, E. Bersin, D. Englund
Sponsorship: NSF, U.S. Army Research Laboratory

The central goal of quantum communication is to deliver quantum information in a way that is resilient against eavesdropping. One notable approach is the measurement-device-independent quantum key distribution (MDI-QKD) protocol, in which a secret key is shared between two parties connected by quantum and classical channels. Essential to this architecture, however, is the ability to faithfully transfer quantum states between two distant qubits. Here, we propose an integrated photonics device for mapping qubits encoded in the polarization of a photon onto the spin state of a cavity-coupled artificial atom: a "polarization-encoded photon-to-spin interface" (PEPSI). We perform theoretical analysis of the state fidelity's dependence on the device's polarization extinction ratio and atom-cavity cooperativity. Furthermore, we explore the rate-fidelity trade-off through analytical and numerical models. In simulation, we show that our design enables efficient, high-fidelity photon-to-spin mapping.

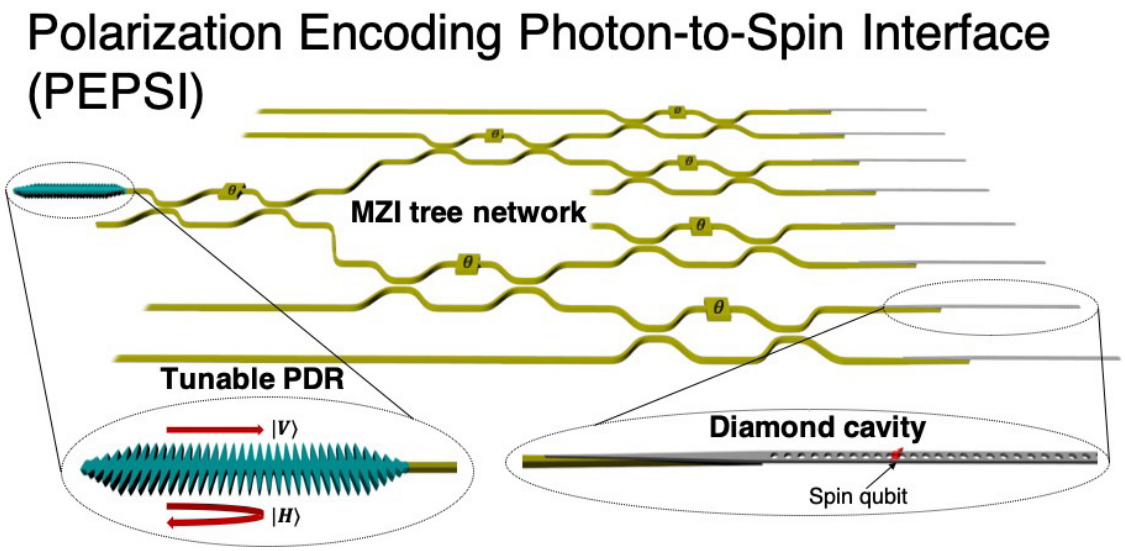

▲ Figure 1: Polarization encoding photon-to-spin interface (PEPSI) consisted of a polarization-selective photonic crystal mirror, a Mach-Zehnder interferometer (MZI) tree network, and an array of integrated diamond nanophotonic cavities in a photonic integrated circuit (PIC). The system includes active phase shifters that permit arbitrary spatial routing of single photons.

FURTHER READING:

- H.-K. Lo, M. Curty, and B. Qi, "Measurement-Device-Independent Quantum Key Distribution," *Phys. Rev. Lett.* 108, 130503, 2012.
- S. L. Braunstein and S. Pirandola, "Side-Channel-Free Quantum Key Distribution," *Phys. Rev. Lett.* 108, 130502, 2012.

Reliability of AlInGaP-on-Si Light-Emitting Diodes

W. A. Sasangka, Y. Gao, K. H. Lee, B. Wang, C. L. Gan, C. V. Thompson
Sponsorship: SMART

Micro-sized light-emitting diodes (μLEDs) are emerging candidates for next-generation microdisplays. To achieve high resolution, it is preferable to integrate red, green, and blue self-emissive LEDs with a Si-complementary metal-oxide-semiconductor (CMOS) driver within a single die using a monolithic CMOS-compatible process. Therefore, fabrication of AlInGaP (for red emission) and InGaN (for blue and green emission) LEDs directly on Si substrates is of great interest.

We have reported on the reliability of InGaN on Si LEDs in previous years. Similar to InGaN on Si, the mismatch in lattice constant between AlInGaP and Si is large, so it is very challenging to grow high-quality AlInGaP on Si. AlInGaP layers on germanium-on-insulator (GOI) on Si substrates with a threading dislocation density of ~1.2x10^{-6} cm^2 have recently been made using wafer bonding and layer transfer techniques.

We have conducted constant current stressing of AlInGaP-on-Si LEDs made using this process by measuring the light intensity over time. Four stages of degradation of the light emission were observed (Figure 1(a)), and the degradation was seen to be non-uniform across the devices (Figure 2). The rate and degree of degradation are seen to be strongly dependent on the stressing current. The initial increase of light emission in stage I is due to the carbonization of organic hydrocarbon residues. These carbonized residues enhance current spreading and therefore increase the light emission. The stage II and III degradation is caused by the oxidation of the top C-doped p-GaAs layer by organic residues. No structural degradation is observed in the multiple quantum well layers. Finally, as the oxidation increases the contact resistance, the applied voltage also increases to keep the stressing current constant, leading to the avalanche breakdown of the contact, which is indicated as stage IV in Figure 1.

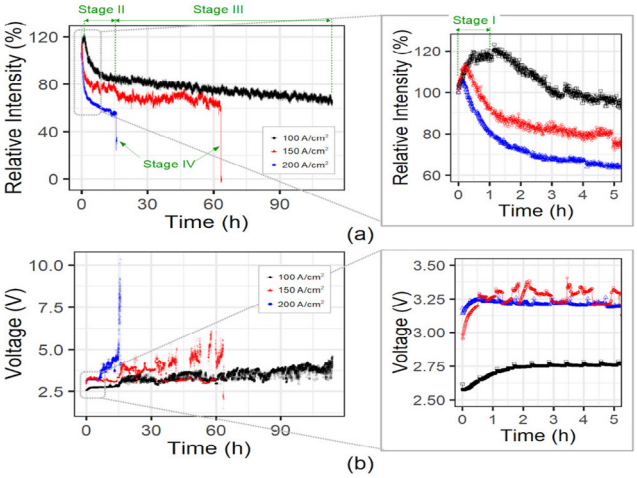

▲Figure 1: Optical and electrical properties of LEDs stressed at different current densities: (a) Relative optical intensity vs time. (b) Applied voltage vs time.

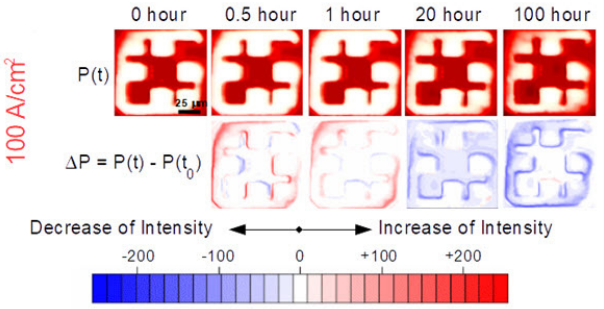

▲Figure 2: Spatial distribution of light intensity of LED stressed at 100 A/cm2. P(t) is a snap-shot taken at a time t during stressing. ΔP is the difference of snapshot at time t with initial snapshot at t = 0.

FURTHER READING

- Y. Wang, B. Wang, W. A. Sasangka, S. Bao, Y. Zhang, H. V. Demir, J. Michel, K. E. K. Lee, et al., "High-performance AlGaInP Light-emitting Diodes Integrated on Silicon through a Superior Quality Germanium-on-insulator," *Photon. Res.*, vol. 6, pp. 290-295, 2018.
- R. I. Made, G. Yu, G. J. Syaranamual, W. A. Sasangka, L. Zhang, X. S. Nguyen, Y. Y. Tay, J. S. Herrin, et al., "Characterization of Defects Generated During Constant Current InGaN-on-Silicon LED Operation," *Microelectronics Reliability*, vol. 76–77, pp. 561, 2017.

Enhancing SiN Waveguide Optical Nonlinearity via Hybrid Gallium Sulfide Integration

S. Deckoff-Jones, V. Pelgrin, J. Zhang, C. Lafforgue, L. Deniel, S. Guerber, R. Ribeiro-Palau, F. Boeuf, C. Alonso-Ramos, L. Vivien, J. Hu, S. Serna
Sponsorship: NSF Graduate Research Fellowship Program, Chateaubriand Fellowship

Silicon nitride (SiN) has become an increasingly prevalent material platform for integrated photonic circuits. SiN enables low-loss waveguides, and it is transparent in both visible and near-infrared (0.25 – 4.3 μmμm). In spite of its small nonlinear index, SiN has been a particularly popular platform for chip-based nonlinear photonic applications, such as supercontinuum generation and frequency combs. However, if SiN's nonlinear index could be increased, the intensity threshold for these useful nonlinear processes could be further reduced. The group-III monochalcogenides (MX, M = Ga, In; X = S, Se, Te) are a class of layered van der Waals materials with strong second- and third-order optical nonlinearities. Gallium sulfide (GaS) in particular has a bulk bandgap of 2.5 eV, large enough to make multi-photon absorption at telecom wavelengths negligible. In this work, we create hybrid waveguides that benefit from the low-loss processing of SiN and the large nonlinear index of the group-III monochalcogenides.

Mechanically exfoliated GaS crystals are transferred onto planarized SiN microring resonators. Figure 1a shows an optical microscope image of a uniform GaS flake fully covering a microring resonator and its coupling region. As the simulated optical TE mode profile in Figure 1b shows, due to the large refractive index (2.6) of GaS, the mode from the SiN core is drawn into GaS. To characterize the nonlinear properties of our hybrid waveguide structures, we measure all-optical cross-wavelength modulation in the microring resonator. We measure enhanced all-optical modulation from the GaS up to 10 MHz (limited by equipment) and measure its nonlinear index to be 10 times larger than that of SiN. This work shows the potential for future incorporation of the group-III monochalcogenides in hybrid waveguides for enhanced optical nonlinearities.

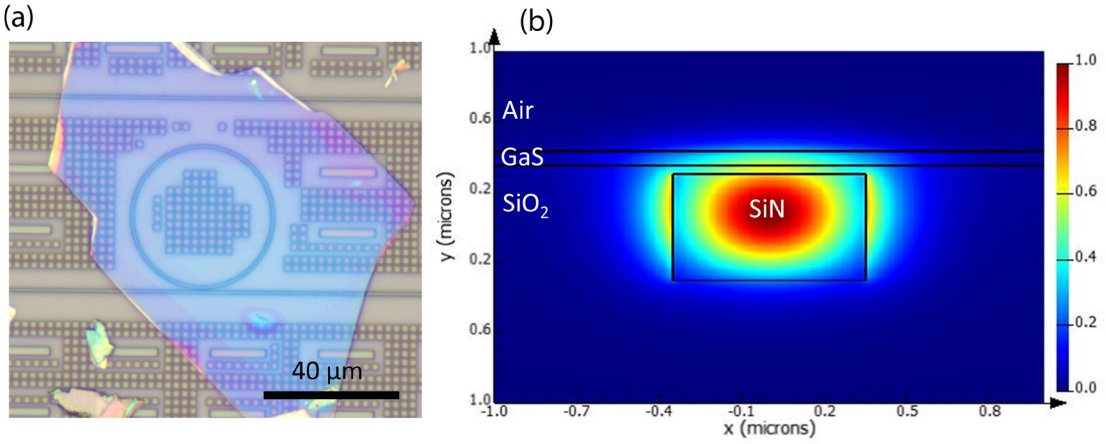

▲ Figure 1: (a) Optical micrograph of SiN microring resonator with mechanically exfoliated GaS flake. (b) Simulated TE mode profile in SiN/GaS hybrid waveguide.

FURTHER READING

- S. Deckoff-Jones, V. Pelgrin, J. Zhang, C. Lafforgue, L. Deniel, S. Guerber, R. Ribeiro-Palau, F. Boeuf, C. Alonso-Ramos, L. Vivien, J. Hu, S. Serna, "Enhancing SiN Waveguide Optical Nonlinearity via Hybrid 2D Material Integration," *J. Opt.* vol. 23, p. 025802, 2021.
- S. Deckoff-Jones, J. Zhang, C. E. Petoukhoff, M. K. L. Man, S. Lei, R. Vajtai, P. M. Ajayan, D. Talbayev, J. Madéo, and K. M. Dani, "Observing the Interplay Between Surface and Bulk Optical Nonlinearities in Thin van der Waals Crystals," *Sci. Rep.* vol. 6, p. 22620, 2016.

Waveguide-Integrated Mid-Infrared Photodetection Using Graphene on a Scalable Chalcogenide Glass Platform

J. Goldstein, H. Lin, S. Deckoff-Jones, M. Hempel, A.-Y. Lu, J. Kong, J. Hu, D. Englund
Sponsorship: MIT Institute for Soldier Nanotechnologies Army University-Affiliated Research Center

The development of compact and fieldable mid-infrared (IR) spectroscopy devices represents a critical challenge for distributed sensing with applications from gas leak detection to environmental monitoring. Greenhouse gases in particular represent an opportunity for IR gas sensing technology, as many of them are relatively inert and cannot be detected by chemical means. Recent work has focused on mid-IR photonic integrated circuit (PIC) sensing platforms and waveguide-integrated mid-IR light sources and detectors based on semiconductors such as PbTe, black phosphorus, and tellurene. However, material bandgaps and reliance on SiO_2 substrates limit operation to wavelengths $\lambda < 4$ µm, whereas the main absorption peaks of the most potent greenhouse gases occur at longer wavelengths. Here we overcome these challenges with a chalcogenide glass-on-CaF_2 PIC architecture incorporating split-gate photothermoelectric graphene photodetectors, shown in Figure 1. Figure 2 plots the photovoltage map of our device, with a maximum responsivity of 1.5 V/W. Our design extends operation to $\lambda = 5.2$ µm with a Johnson noise-limited noise-equivalent power of 1.1 nW/Hz$^{1/2}$ with no fall-off in photoresponse up to $f_{3dB} = 1$ MHz and a predicted 3-dB bandwidth of $f_{3dB} > 1$GHz. This mid-IR PIC platform readily extends to longer wavelengths and opens the door to applications from distributed gas sensing and portable dual comb spectroscopy to weather-resilient free space optical communications.

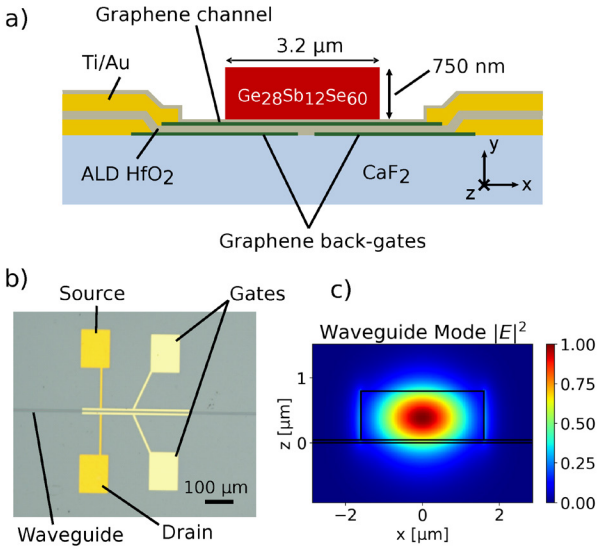

▲ Figure 1: a) Illustration of the device's cross section perpendicular to the waveguide axis. The optical mode supported by the $Ge_{28}Sb_{12}Se_{60}$ waveguide evanescently couples to and is absorbed by the graphene channel, which is gated by two graphene back-gates to induce a p-n junction. b) Optical image of the device depicting source, drain, and gate contact pads. c) Depiction of the optical guided mode at $\lambda = 5.2$ µm.

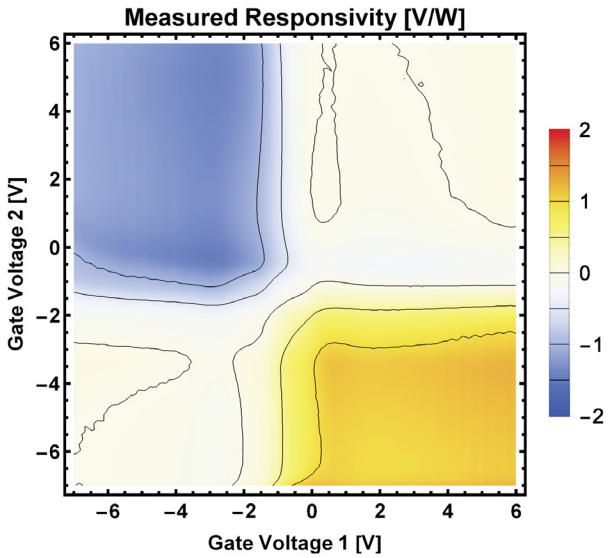

▲ Figure 2: Measured responsivity map of our device as a function of the voltages applied to the two back-gates. The photoresponse pattern indicates a photothermoelectric response mechanism and is qualitatively consistent with the behavior predicted by our device model.

FURTHER READING

- A. Yadav and A. M. Agarwal, "Integrated Photonic Materials for the Mid-Infrared," *International Journal of Applied Glass Science*, vol. 11, pp. 491-510, 2020.

Imaging Transparent Objects through Dynamic Scattering Media Using Recurrent Neural Networks

I. Kang, S. Pang, Q. Zhang, N. Fang, G. Barbastathis
Sponsorship: Intelligence Advanced Research Projects Agency, Korea Foundation for Advanced Studies

Transparent objects in biological imaging and X-ray imaging are imaged by solving inverse problems based on their diffraction intensity patterns. However, the scattering process induced by their complex interiors complicates inverse problems with a severity depending on the statistics of the refractive index gradient and contrast profiles. Recently, static neural networks were used to retrieve original information from the scattering. Here, we propose a novel dynamical machine learning approach to image phase objects through dynamic diffusers. The motivation of this study is to accommodate the input with spatiotemporal dynamics, such as a temporal recording of time-varying scattering profiles. This dynamical machine learning architecture is adopted to strengthen and exploit the correlation among adjacent scattering patterns during the training and testing processes. To impart dynamics, we propose a simplified dynamical model as follows. We use the on-axis rotation of a diffuser and utilize multiple speckle measurements from different angles to form a sequence of images for training. Our recurrent neural network (RNN) architecture effectively discards any redundancies and enhances/filters out the static pattern, that is, the quantitative phase information of transparent objects. This method is also applicable to other imaging applications that involve any other spatiotemporal dynamics.

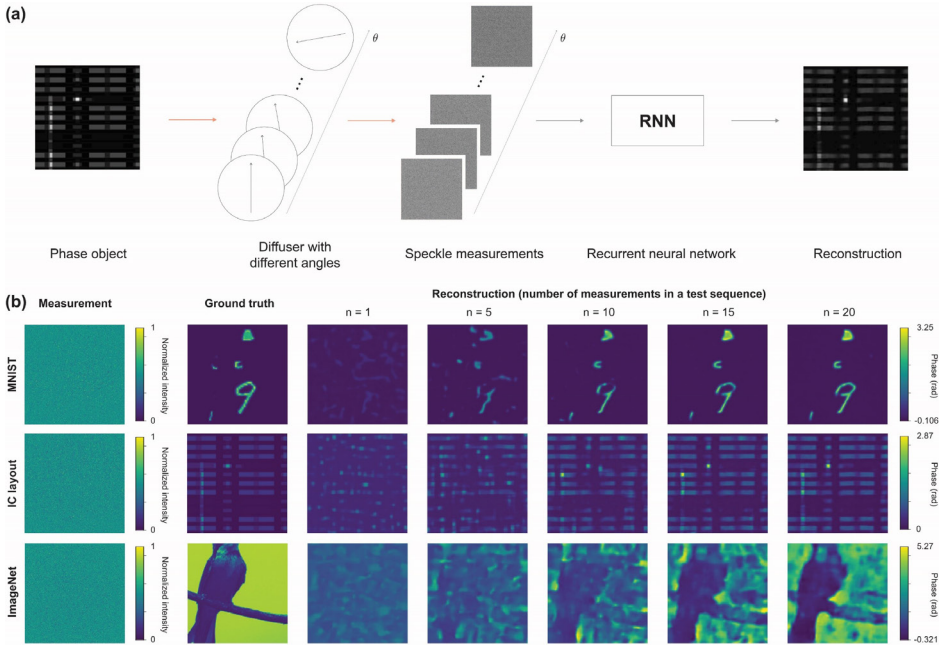

▲ Figure 1: (a) Collimated beam illuminates a phase object, and the diffracted optical field is strongly scattered by a diffuser, which is rotated on-axis for several different angles. For each angle of rotation, a camera records speckle measurements; they are processed by our proposed RNN architecture, hence the reconstruction. (b) Seen angles of the rotation with unseen phase objects. Qualitatively shown are the progressions of reconstructions according to the number of measurements in a test sequence (n) for three different priors.

FURTHER READING

- S. Li, M. Deng, J. Lee, A. Sinha, and G. Barbastathis, "Imaging Through Glass Diffusers Using Densely Connected Convolutional Networks," *Optica*, vol. 5, no. 7, pp. 803-813, 2018.
- Y. Li, Y. Xue, and L. Tian, "Deep Speckle Correlation: a Deep Learning Approach Toward Scalable Imaging Through Scattering Media," *Optica*, vol. 5, no. 10, pp. 1181-1190, 2018.

Field-Based Design of a Resonant Dielectric Antenna for Coherent Spin-Photon Interfaces

L. Li, H. Choi, M. Heuck, D. Englund
Sponsorship: MITRE, NSF

We propose a field-based design for dielectric antennas to interface diamond color centers in dielectric membranes with a Gaussian propagating far field. This antenna design enables an efficient spin-photon interface with a Purcell factor exceeding 400 and a 93% mode overlap to a 0.4 numerical aperture far-field Gaussian mode. The antenna design with the back reflector is robust to fabrication imperfections, such as variations in the dimensions of the dielectric perturbations and the emitter dipole's location. The field-based dielectric antenna design provides an efficient free-space interface to closely packed arrays of quantum memories for multiplexed quantum repeaters, arrayed quantum sensors, and modular quantum computers.

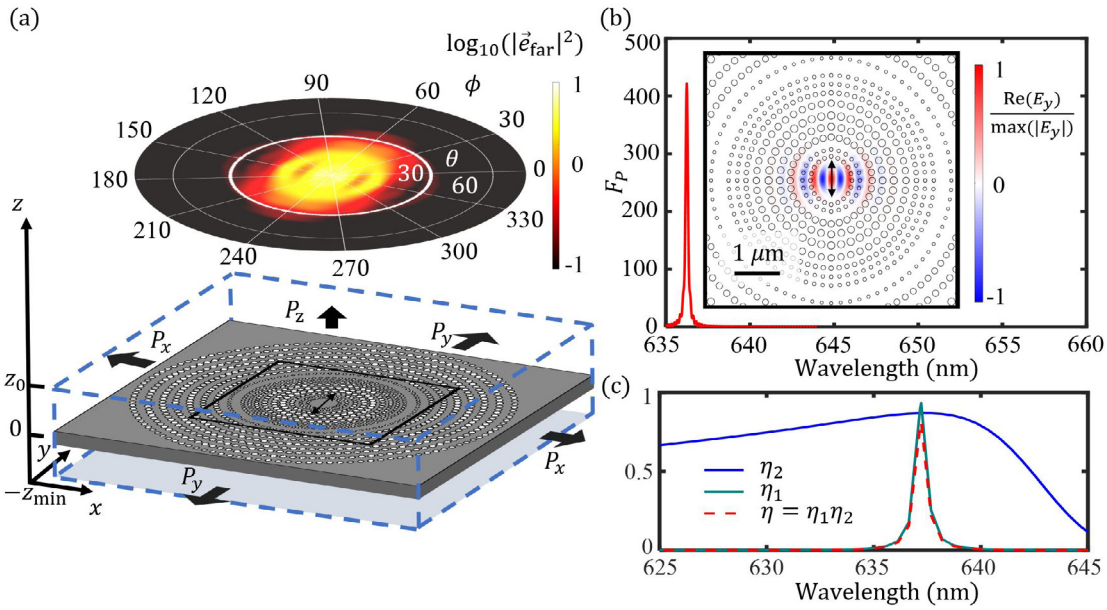

▲ Figure 1: (a) Illustration of the dielectric antenna structure, along with a far-field distribution plot. (b) Purcell factor spectrum of the antenna structure. The inset is a linear-scale plot of normalized electric field corresponding to the black square region in (a). (c) The spin-photon interface efficiency eta, spin-antenna interface efficiency eta1, and antenna efficiency eta2 as the function of wavelength of the antenna structure in (a).

FURTHER READING:

- L. Li, H. Choi, M. Heuck, and D. Englund, "Field-based Design of a Resonant Dielectric Antenna for Coherent Spin-photon Interfaces," *Opt. Express* 29, 16469 (2021).
- L. Li, H. Choi, M. Heuck, and D. Englund, "Field-based Design of a Resonant Dielectric Antenna for Coherent Spin-photon Interfaces," 2021 *Conference on Lasers and Electro-Optics (CLEO)*, 2021, pp. 1-2.

Strategies for High-Performance Solid-State Photon Upconversion Based on Triplet Exciton Annihilation

T.-A. Lin, C. F. Perkinson, M. Wu, J. O. Tiepelt, V. Bulović, M. A. Baldo
Sponsorship: DoE

Photon upconversion, a non-linear optical process to convert low-energy photons into higher energies, has various applications such as photovoltaics, infrared sensing, and bio-imaging. In particular, upconversion based on triplet exciton annihilation is one of the most promising approaches to achieve high efficiency at low excitation intensity for practical applications. However, the reported performance in solid-state is limited due to energy back transfer, materials aggregation, and weak optical absorption, which complicates the integration with solid-state applications (Figure 1).

Here, we propose strategies to improve the performance in solid-state via device structure engineering. In a green-to-blue upconverter consisting of a bilayer of an absorbing and an upconverting material, we reduce energy back transfer by inserting a blocking layer in between and mitigate aggregation by doping the absorber into a host material. The upconversion efficiency had a 7-fold enhancement, with the excitation intensity reduced by 9 times (Figure 2a). To improve optical absorption, we investigate an infrared- to-visible upconverter and integrate the upconverting layers into a Fabry-Pérot microcavity. At the resonant wavelength, infrared absorption increases 74-fold, and the threshold excitation intensity for upconversion is reduced by two orders of magnitude to a sub-solar flux (Figure 2b). Our work demonstrates the importance of device structure engineering to improve the performance of solid-state photon upconversion and offers a path towards practical applications.

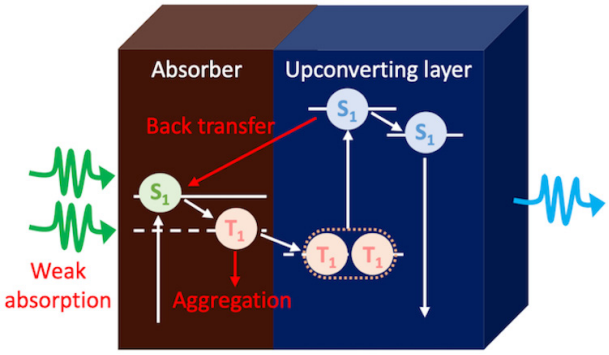

◀Figure 1: Schematic of a solid-state triplet excitonic upconverter out-lining the three major loss pathways.

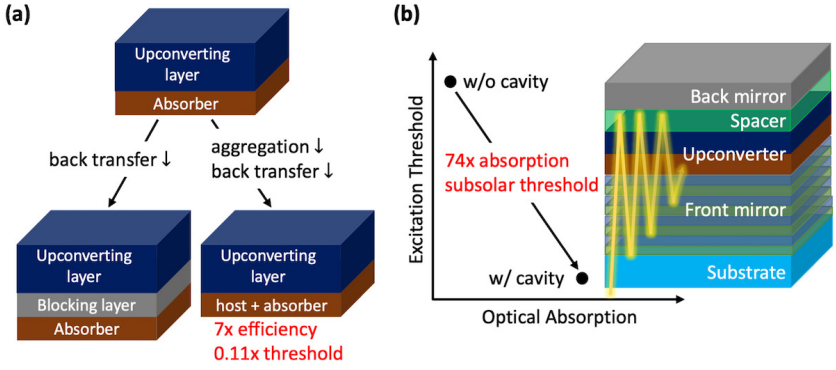

▼Figure 2: Device structure designs for (a) mitigating back transfer and aggregation and (b) enhancing optical absorption.

FURTHER READING

- T.-A. Lin, C. F. Perkinson, and M. A. Baldo, "Strategies for High-Performance Solid-State Triplet-Triplet-Annihilation-Based Photon Upconversion," *Advanced Materials*, vol. 32, no. 26, p. 1908175, 2020.
- M. Wu, T.-A. Lin, J. O. Tiepelt, V. Bulović, and M. A. Baldo, "Nanocrystal-Sensitized Infrared-to-Visible Upconversion in a Microcavity under Subsolar Flux," *Nano Letters*, vol. 21, no. 2, p. 1011, 2021.

Magnet Field-Switchable Laser via Optical Pumping of Rubrene

C. F. Perkinson, M. Einzinger, J. Finley, M. G. Bawendi, M. A. Baldo
Sponsorship: Department of Energy, NSF Graduate Research Fellowship

Optical imaging of magnetic fields is used in spintronics, magnetic resonance imaging, and radiology. Most conventional approaches to magnetic field imaging rely on expensive crystalline materials or garnets, but the cost of these materials makes them poorly suited to high-area imaging. Magnetic sensing applications may benefit from cheaper magnetically active dyes. We demonstrate that the well-studied organic molecule rubrene can be used to spatially resolve magnetic fields. Furthermore, we report a 460% enhancement in rubrene brightness under a 0.4-T magnetic field in a first-of-its-kind magnetic field-switchable laser. We attribute the high magnetic sensitivity of rubrene to the magnetic field dependence of singlet fission, a process whereby one spin-singlet excitation splits into two spin-triplet excitations. These results suggest that rubrene—and other organic molecules that exhibit singlet fission—are promising candidates for low-cost, high-sensitivity magnetic imaging.

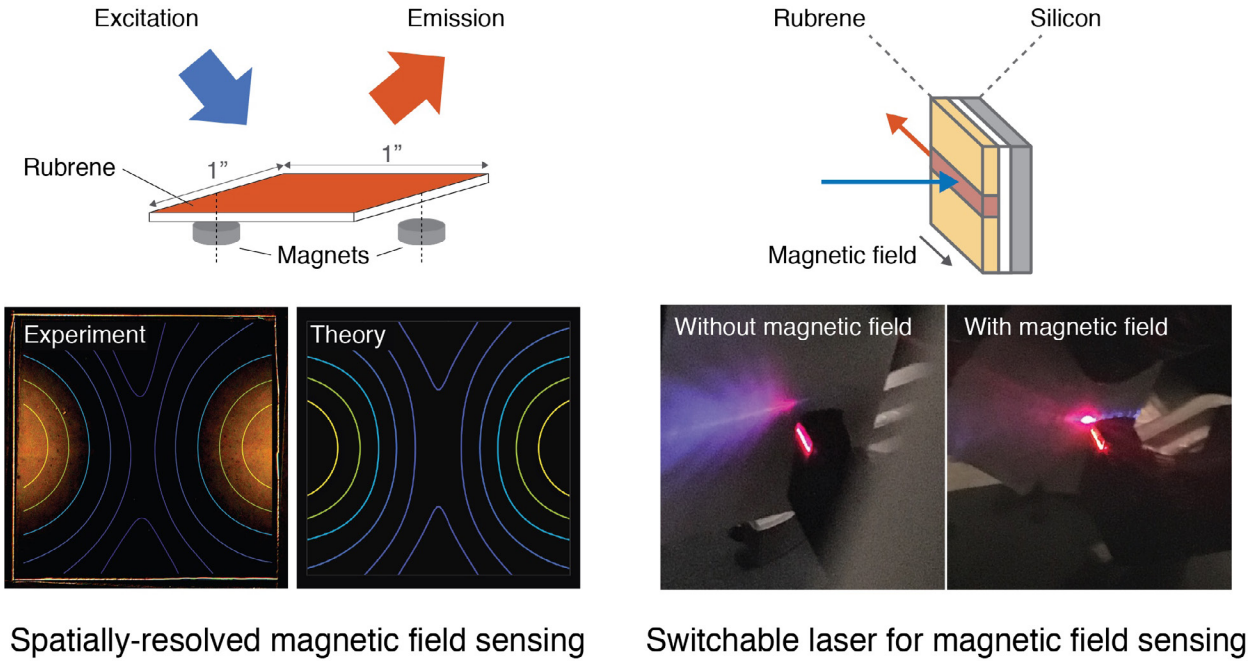

▲ Figure 1: (Left) Spatially resolved magnetic field sensing through modulation of rubrene emission intensity. (Right) Optically pumped waveguide laser, showing magnetic field switching between non-lasing and lasing modes.

Multiplexed Raman Sensors Using Swept-Source Excitation

N. Persits, J. Kim, Z. Li, R. Ram
Sponsorship: Food and Drug Administration (FDA)

Spontaneous Raman spectroscopy is routinely used in pharmaceutical production, chemical analysis, and the semiconductor industry for characterization of structural features, strain, and doping. Standard Raman systems require dispersive spectrometers and often specialized cooled charge-coupled device (CCD) detectors to compensate for the low signals, making them prohibitively expensive and bulky. In this work we introduce and demonstrate a novel Raman system architecture using a swept-source laser excitation, replacing the spectrometer. The laser is delivered through optical fibers to custom-made Raman probes, which are designed to be compatible with either single-mode or telecom-standard multimode optical fibers. Each probe delivers the excitation light onto a sample and collects the Raman signal, which is then detected using a narrow optical filter in front of a room-temperature high-gain Si photodiode. With a standard telecom optical switch, we can multiplex up to 16 channels and deploy remote probes using an optical fiber network. As an initial proof-of-concept, we present the spectra collected with our probes for both solid polystyrene and liquid urea solutions and further show that the acquired spectra have signal-to-noise ratios comparable to that collected with our lab-built bench top Raman system. We believe this new system, in which a single tunable laser can serve a distributed sensor network, significantly reduces the space and cost of current spectrometer-based Raman systems and promotes the use of Raman for online process control.

Hafnia-Filled Photonic Crystal Emitters for Mesoscale Thermophotovoltaic Generators

R. Sakakibara, V. Stelmakh, W. R. Chan, R. Geil, M. Ghebrebrhan, J. D. Joannopoulos, M. Soljačić, I. Čelanović
Sponsorship: U.S. ARO, DOE

Thermophotovoltaic (TPV) systems are promising as small-scale, portable generators for power sensors, small robotic platforms, and portable computational and communication equipment. In TPV systems, an emitter at high temperature emits radiation that is then converted to electricity by a low- bandgap photovoltaic cell. One way to increase both TPV power and efficiency is to use two-dimensional, hafnia-filled-and-capped tantalum photonic crystals (PhCs); they enable spectral tailoring of thermal radiation for a wide range of angles. However, two key features are hard to realize simultaneously: a uniformly filled cavity and a thin capping film. Cavity-filling leads to a capping film that is both thick and uneven, so that trying to thin the film removes hafnia from within the cavity. Here, we present a method to reduce the film roughness and better control the thickness. Improved PhCs can pave the way toward high-performance TPV micro-generators for off-the-grid applications.

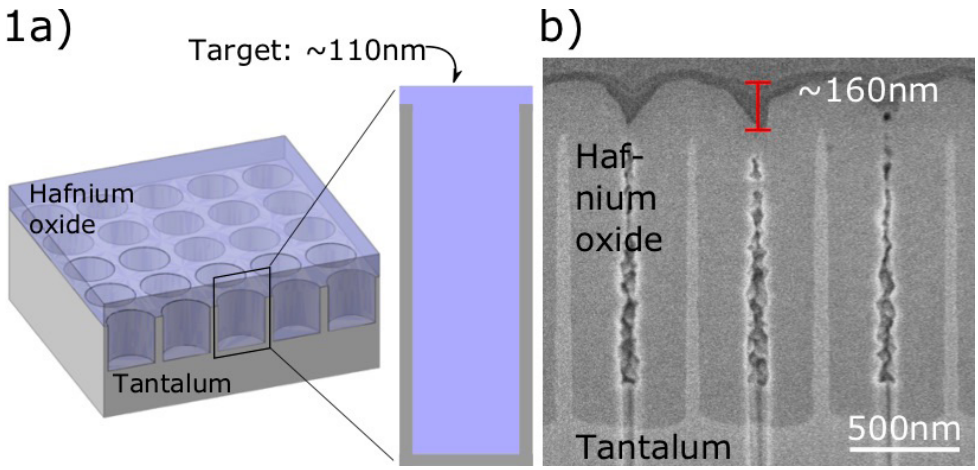

▲Figure 1: a) The ideal filled PhC should have a flat and thin capping layer. b) The fabricated PhC cross section shows a thick and uneven capping film.

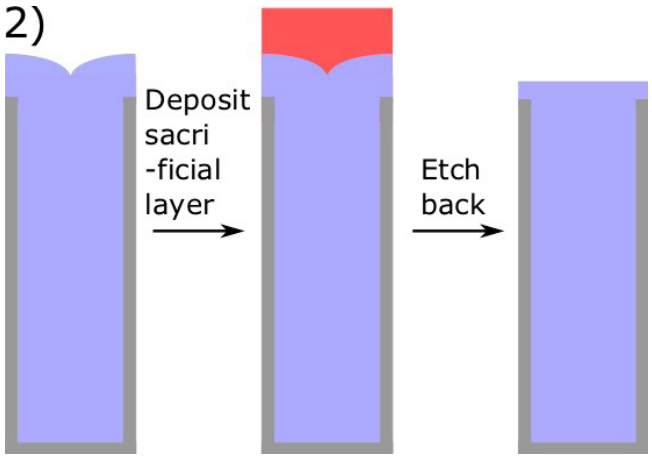

◀Figure 2: A planarization and etch back process is used to reduce both roughness and thickness.

FURTHER READING

- W. R. Chan, V. Stelmakh, M. Ghebrebrhan, M. Soljačić, J.D. Joannopoulos, and I. Čelanović, "Enabling Efficient Heat-to-electricity Generation at the Mesoscale," *Energy Environ. Sci.*, vol. 10, pp. 1367-1371, 2017.
- Y. X. Yeng, J. Chou, V. Rinnerbauer, Y. Shen, S.-G. Kim, J. D. Joannopoulos, M. Soljačić, and I. Čelanović, "Global Optimization of Omnidirectional Wavelength Selective Emitters/absorbers Based on Dielectric-filled Anti-reflection Coated Two-dimensional Metallic Photonics Crystals," *Opt. Express*, vol. 22, pp. 21711-21718, 2014.

High-Performance Non-Mechanically-Tunable Meta-Lens

M. Y. Shalaginov, S. An, Y. Zhang, F. Yang, P. Su, V. Liberman, J. B. Chou, C. M. Roberts, M. Kang, C. Rios, Q. Du, C. Fowler, A. Agarwal, K. Richardson, C. Rivero-Baleine, H. Zhang, J. Hu, T. Gu
Sponsorship: Defence Advanced Research Projects Agency Extreme Optics and Imaging (EXTREME) Program

Optical metasurfaces, i.e., ultra-thin arrays of sub-wavelength antennae, have enabled a new range of photonic devices with unprecedented functionalities in sculpting wavefronts and a substantially reduced form-factor. Recently special interest has been drawn to a class of so-called "active metasurfaces," whose optical properties can be modulated post-fabrication by non-mechanical effects. A variety of tuning mechanisms have been harnessed; however, demonstrated meta-optical devices often incur narrow tuning ranges and low optical efficiencies. Here, we implemented an active varifocal meta-lens based on phase-change materials that offers 1) aberration-free performance across arbitrary optical states; 2) extremely low crosstalk of nearly 30 dB; and 3) considerably enhanced focusing efficiency exceeding 20% in both states with a clear pathway for further improvement. This advancement will further unveil a new cohort of exciting applications of active metasurfaces in imaging, sensing, display, and optical ranging.

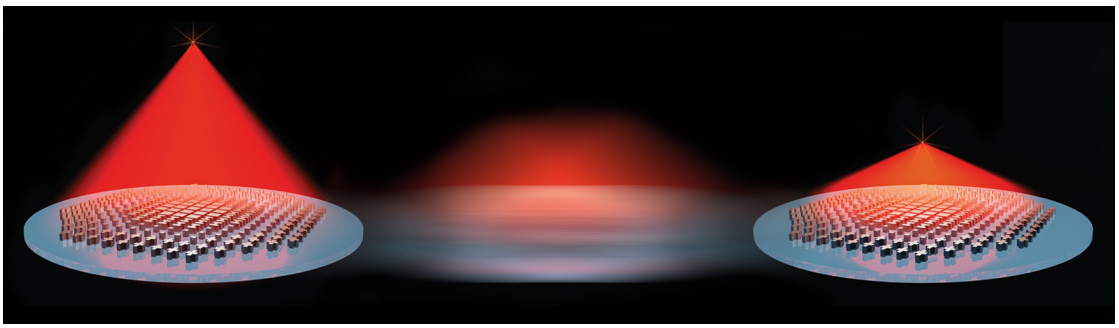

▲ Figure 1: Illustration of a non-mechanically-actuated varifocal meta-lens made of phase-change material (Ge2Sb2Se4Te1). Focal plane position is switched between the two states depending on the optical material state (amorphous or crystalline).

GaN µLEDs for Microsystem Optical Communications

S. Spector, M. Hempel, T. Palacios
Sponsorship: AFOSR, MIT Experiential Learning Opportunity

Electronic systems smaller than 50 µm are promising for ubiquitous sensing; however, wireless communication with such systems is challenging since radio-frequency communication is inefficient at the micron scale. Small length scales motivate the use of optical communications for micro-devices, which must be low-power due to the size constraint on solar cell surface area. Here we present an analysis of blue GaN microLEDs (µLEDs) for optical communications with 50 x 50 µm² sensor microsystems called SynCells. We analyzed µLEDs with sizes from 5 x 10 µm² up to 150 x 150 µm², developing a test setup that can detect an LED driven by only 1 nW (Figure 1). We found higher external quantum efficiency (EQE) for larger µLEDs; also, EQE increased with current density up to a peak value, after which we observed an efficiency droop resulting from Auger recombination. GaN µLEDs operating at maximally efficient current density will be able to produce detectable optical signals at sufficiently low power for practical use in SynCells.

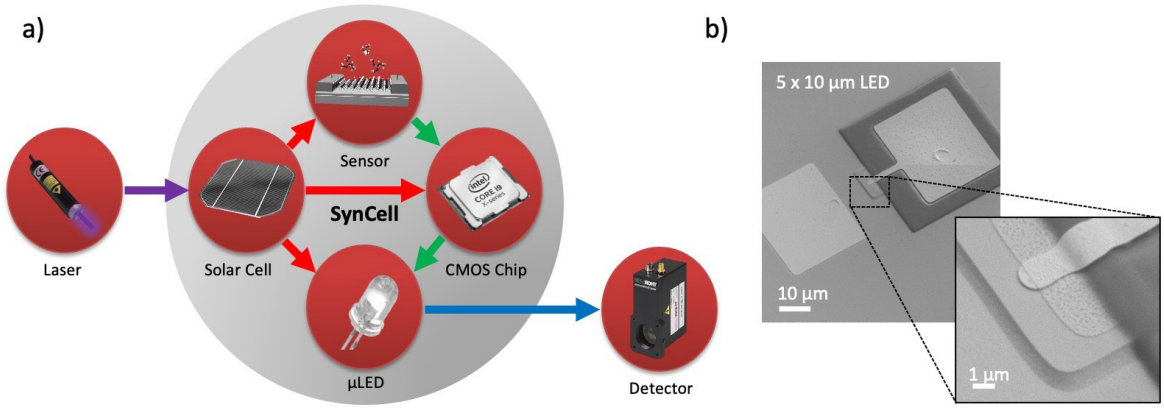

▲Figure 1: a) Block diagram of SynCell operation including µLED and photomultiplier tube detector for optical communication; b) SEM image of a 5 x 10 µm2 GaN µLED.

Large-area Optical Metasurface Fabrication using Nanostencil Lithography

P. Su, M. Shalaginov, T. Gu, S. An, D. Li, L. Li, H. Jiang, S. Joo, L. C. Kimerling, H. Zhang, J. Hu, A. Agarwal
Sponsorship: DARPA

Optical metasurfaces promise optical components with on-demand control of light and reduced size, weight, and power (SWaP) compared to their bulk counterparts. However, fabrication of metasurfaces in the optical spectral range often relies on electron beam lithography due to the high resolution requirements, which makes fabrication scale poorly with the device dimensions. Recently, deep ultraviolet (DUV) lithography has been validated as a scalable manufacturing route for optical metasurfaces. However, DUV lithographic fabrication requires significant capital investment and is also limited to standard materials and processes available in foundries.

We are developing nanostencil lithography as an alternative technique for scalable, versatile, and rapid prototyping of metasurface devices. Nanostencils are nano-scale shadow masks, which allow repeated fabrication of a pattern via any anisotropic deposition process once the nanostencil is made. Previous research that used nanostencil lithography required only deposition of very thin layers (100 nm or less) through the nanostencil, while transmissive dielectric metasurfaces require significantly thicker layers, especially as the wavelength of light increases. Previous nanostencils were also limited to 1 mm by 1 mm in size. We improved previous processes for fabricating and using nanostencils, increasing the yield of nanostencil fabrication by not fully etching through the nanostencil membrane before the KOH etch and improving the consistency of metasurface fabrication by developing a resist-based spacer layer. Figure 1 outlines the resulting processes.

To show the effectiveness of nanostencil lithography for large-area optical metasurface fabrication, we used 2 mm by 2 mm nanostencils to fabricate 1.5-mm-diameter PbTe metalenses on CaF_2. The lenses showed diffraction-limited focusing, with a representative focal spot shown in Figure 2, and focusing efficiencies comparable to efficiencies reported in state-of-the-art large-area dielectric metalenses.

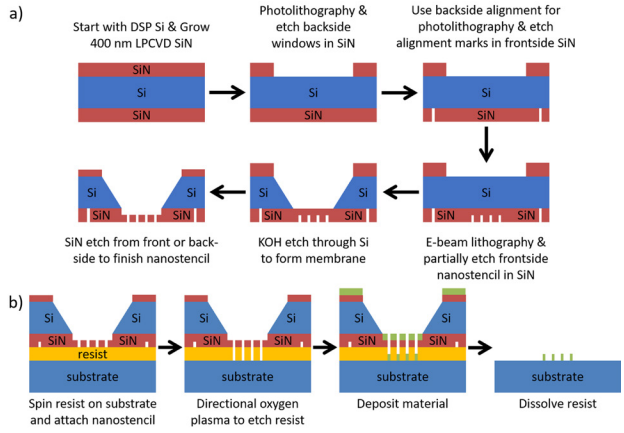

▲Figure 1: Schematics of (a) the fabrication process for large-area silicon-nitride-based nanostencils and (b) the process for using nanostencils on rigid substrates.

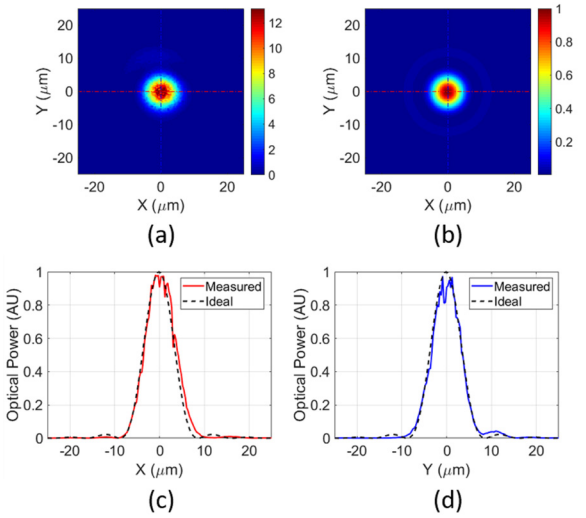

▲Figure 2: Representative (a) measured and (b) simulated images, along with the (c) x-axis and (d) y-axis cross sections of the focal spot of a metalens fabricated using nanostencils.

FURTHER READING

- P. Su, M. Shalaginov, T. Gu, S. An, D. Li, L. Li, H. Jiang, S. Joo, L. C. Kimerling, H. Zhang, J. Hu, and A. Agarwal, "Large-area Optical Metasurface Fabrication Using Nanostencil Lithography," *Optics Letters*, vol. 46, no. 10, pp. 2324-2327, May 2021.
- P. Su, K. Stoll, M. Shalaginov, T. Gu, S. An, D. Li, L. Li, H. Jiang, S. Joo, L. C. Kimerling, H. Zhang, J. Hu, and A. Agarwal, "Nanostencil Lithography for Scalable Optical Metasurfaces," to be presented at *OSA Optical Design and Fabrication Congress*, online, June 2021.
- P. Su, "Lead Chalcogenide Thin Film Materials and Processing for Infrared Optical Devices," *Ph.D. dissertation*, Massachusetts Institute of Technology, Cambridge, 2020.

The Effect of O:N Ratio in a HfOxNy Interlayer on Triplet Energy Transfer In Singlet-Fission-Sensitized Silicon

C. F. Perkinson*, N. Wong*, M. A. Baldo
*These authors contributed equally to this work
Sponsorship: DOE

With the climate changing, the Sun is a promising source of renewable energy. However, silicon photovoltaics, the current industry standard, are approaching their theoretical efficiency limit. A proposed method to exceed this limit is to sensitize silicon with a material that undergoes singlet exciton fission, a carrier multiplication process with the potential to reduce thermalization losses by creating two excited electrons from a single photon. Successful transfer of these two electrons to silicon could result in increased photocurrent and improved device efficiency. Recently, our group demonstrated the first proof-of-concept solar cell incorporating tetracene as a singlet fission material to produce additional carriers that are transported to silicon via a thin layer of hafnium oxynitride (HfO_xN_y). With the aim of improving singlet-fission-sensitized silicon solar cells, our research focuses on understanding what properties are necessary for the transport layer between singlet fission materials and silicon and the mechanism for the energy transfer process. In this work, the defect density of a HfO_xN_y interlayer is varied by changing the oxygen-to-nitrogen ratio, and different interlayer thicknesses are studied to examine the role of defect states on energy transfer from tetracene to silicon. The transfer efficiency is inferred via magnetic field modulation of the silicon photoluminescence. The results form a preliminary basis for unravelling the exciton transfer mechanism, which will subsequently be studied using time-resolved spectroscopy. Ultimately, knowledge of interlayer material properties and insights into the mechanism of energy transfer to silicon may inform the design of sensitizing layers for silicon and pave the way to commercializing the use of singlet fission to boost silicon photovoltaic efficiencies.

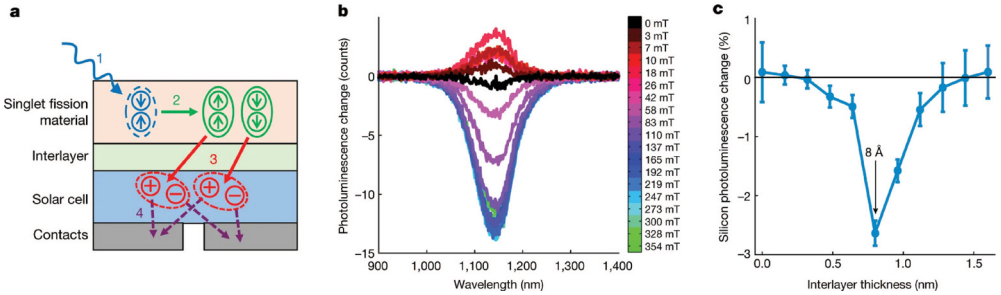

▲ Figure 1: a) Schematic of a singlet-fission-sensitized solar cell, b) applying a magnetic field changes the efficiency of singlet fission, which is observable as a change in silicon photoluminescence, c) singlet fission sensitization is maximized using a HfOxNy interlayer thickness of 8Å.

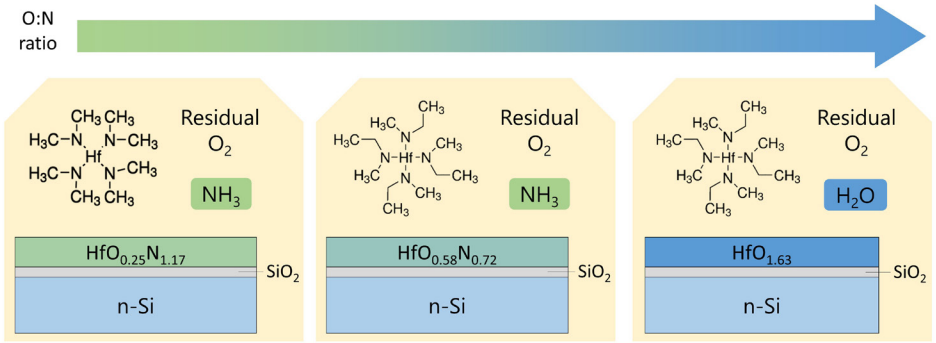

▲ Figure 2: The choice of precursors used in atomic layer deposition modifies the O:N atomic ratio in a passivating layer of HfOxNy.

FURTHER READING

- M. Einzinger, T. Wu, J. F. Kompalla, H. L. Smith, C. F. Perkinson, L. Nienhaus, S. Wieghold, D. N. Congreve, et al., "Sensitization of Silicon by Singlet Exciton Fission in Tetracene," *Nature*, vol. 571, pp. 90-94, 2019. [Online.] Available: https://www.nature.com/articles/s41586-019-1339-4.

LION: Learning to Invert 3D Objects by Neural Networks

G. Barbastathis, J. Song, Z. Wu, I. K. S. Pang, Z. Guo
Sponsor: IARPA RAVEN (Rapid Analysis of Various Emerging Nanoelectronics)

Non-destructive three-dimensional imaging is important to establish the internal structure of a 3D object non-invasively. In our work, objects of interest are integrated circuits (ICs). This operation requires sufficient measurements for computational reconstruction, such as measurements from different angles or depths. Meanwhile, if the required acquisition time is too long, the operation may become impractical, not to mention the risk of instabilities or even damage to the samples from X-ray radiation. Reducing the number of angular views and the radiation dosage per view can be used to limit beam exposure, but low-dose data acquisition schemes yield noisy measurements that significantly reduce the quality of the reconstructed image.

Our goal in this project is to reduce the acquisition time by a factor of 10 100 through augmenting image reconstruction with machine learning. In the LION approach, we embed the physics of X-ray propagation and interaction with matter into the learning process. This improves both the fidelity and the efficiency of learning. We study two types of information-starved 3D imaging: limited-angle tomography and low-dose tomography. A limited-angle tomography combined with an advanced ptychography technique, achieves high-resolution (10 nm) reconstruction with the advanced technique of recurrent neural network and generative adversarial network (see Figure 1a, b). On the other hand, low-dose tomography suffers from shot noise as the photon budget reduces (<50 photons per ray). Regardless of 20 of reduction in photon budget for 50 photons case, the physics-assisted machine learning still reconstructs ICs with high fidelity (Test PCC: 0.80) (see Figure 1c).

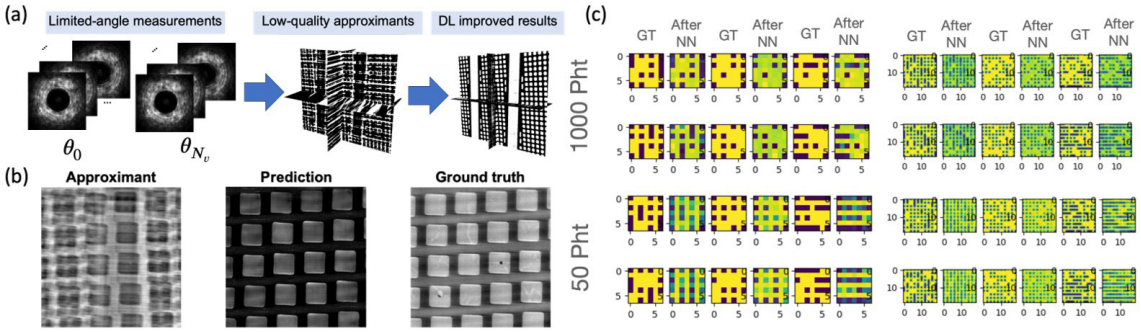

▲ Figure 1: (a) Deep learning-based 3D volume reconstruction framework for limited-angle tomography. (b) Deep learning-based reconstruction results in terms of low-quality approximants, deep learning-based reconstruction results, and ground truth from sufficient measurements. (c) Reconstruction ICs (7 ×7 × 5, left and 19 × 19 × 5, right) from low-dose tomography with reducing photon counts per ray (from 1000 to 50).

FURTHER READING

- Kang, I., Goy, A., and Barbastathis, G. (2021). "Dynamical Machine Learning Volumetric Reconstruction of Objects' Interiors from Limited Angular Views," *Light: Science & Applications*, 10(1), 1-21.
- Goy, A., Rughoobur, G., Li, S., Arthur, K., Akinwande, A. I., & Barbastathis, G. (2019). "High-resolution Limited-angle Phase Tomography of Dense Layered Objects Using Deep Neural Networks," *Proceedings of the National Academy of Sciences*, 116(40), 19848-19856.

Light Sources and Single-Photon Detectors in Bulk CMOS

J. Xue, J. Kim, A. Mestre, K. M. Tan, D. Chong, S. Roy, H. Nong, K. Y. Lim, D. Gray, D. Kramnik, A. Atabaki, E. Quek, R. J. Ram
Sponsorship: GlobalFoundries, A*STAR, Kwanjeong Educational Foundation

Silicon photonics realized in complementary metal-oxide semiconductor (CMOS) processes has transformed computing, communications, sensing, and imaging. Here, we demonstrate a chip-to-chip fiber optic link that implements both the light source and detector in bulk CMOS. A high-brightness infrared light emission in forward bias for a silicon p-n junction is implemented in an open-foundry CMOS process – 55 BCDLite. Emission intensity of 50 mW/cm^2 light at a wavelength of 1020 nm is realized at room temperature by using a deep vertical junction with lightly doped rings.

An infrared-enhanced single photon avalanche diode (SPAD) was designed in the same process and used to collect the 1020-nm light emission. We find that a detector using the p-substrate as part of the p-n junction achieves good detection (6% quantum efficiency for a 20-µm diameter device) even at a wavelength of 1020 nm. This device has a breakdown voltage of -24V and can be operated in Geiger mode to achieve photon detection at low light levels. The capabilities of the two devices combine to demonstrate a complete chip-to-chip optical interconnect utilizing only silicon CMOS devices.

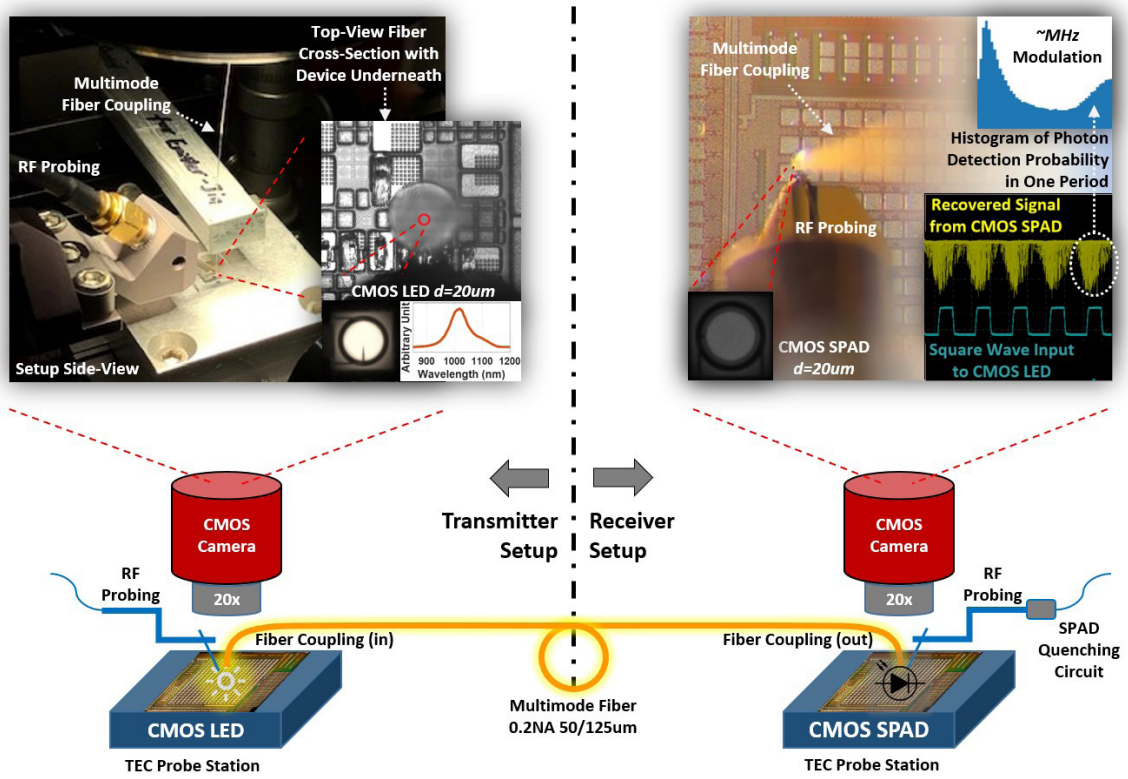

▲ Figure 1: Optical transmission of modulation waveform from CMOS LED to CMOS SPAD over a standard multimode optical fiber.

FURTHER READING

- J. Xue et al., "Low Voltage, High Brightness CMOS LEDs," *2020 IEEE International Electron Devices Meeting (IEDM)*, 2020, pp. 33.5.1-33.5.4, doi: 10.1109/IEDM13553.2020.9371911.

Inference of Process Variations in Silicon Photonics from Characterization Measurements

Z. Zhang, S. I. El-Henawy, C. Ríos, D. S. Boning

Silicon photonics, which manipulates photons instead of electrons, shows promise for higher data rates, lower-energy communication and information processing, biomedical sensing, and novel optically based functionality applications such as wavefront engineering and beam steering of light. In silicon photonics, both electrical and optical components can be integrated on the same chip, using a shared silicon integrated circuit (IC) technology base. However, silicon photonics does not yet have mature process, device, and circuit variation models for the existing IC and photonic process steps; this lack presents a key challenge for design in this emerging industry.

Our goal is to develop key elements of a robust design for manufacturability (DFM) methodology for silicon photonics. One of the key steps for the goal is to find the distribution map of process variation in the actual fabrication, which is usually inferred from well-designed test structure measurements.

In this work, we develop a Bayesian-based method to infer the distribution of systematic geometric variations in silicon photonics that aims to reduce the extraction error caused by measurement noise. We apply this method to characterization data from multiple silicon nitride ring resonators with different design parameters and produce the estimated spatial map of device geometric variations (e.g., waveguide width, Si_3N_4 on SiO_2 thickness, partial etch depth), as shown in Figure 1. Our results show that this characterization scheme can serve as a good test structure for process variation inference. Since characterization measurements are commonly used for device optimization design, our method provides an efficient alternative approach to study process variation in silicon photonics without requiring separate or replicated test structure design and thus facilitates the design of high-yield silicon photonic circuits in the future.

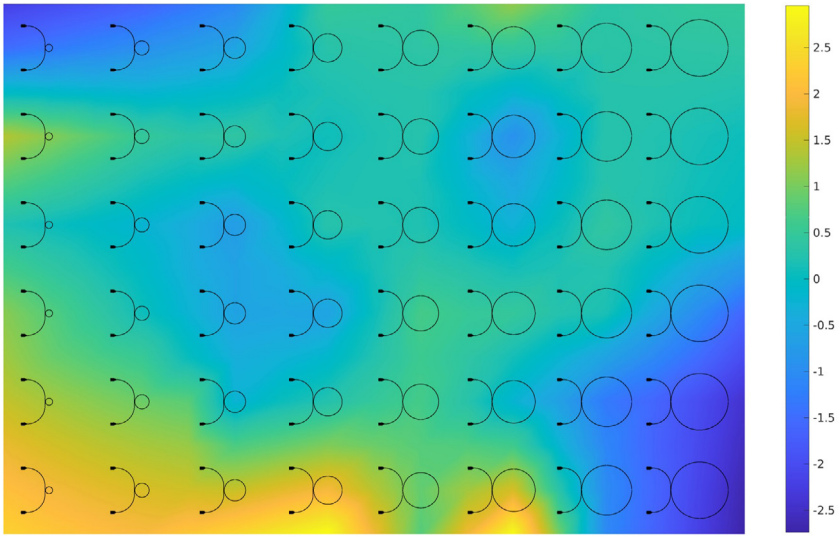

▲ Figure 1: The characterization design layout with our estimation of the Si3N4 on SiO2 thickness variation map inferred from the measurement.

FURTHER READING

- L. Chrostowski and M. Hochberg, "Silicon Photonics Design: from Devices to Systems," Cambridge: Cambridge University Press, 2015.

Integrated Photonics and Electronics for Chip-Scale Control of Trapped Ions

J. Stuart, J. M. Sage, I. L. Chuang, J. Chiaverini
Sponsorship: Under Secretary of Defense for Research and Engineering and Department of Defense, MIT Lincoln Laboratory

Trapped atomic ions are promising candidates for quantum information processing and quantum sensing. Current state-of-the-art trapped-ion systems require many lasers and electronics to achieve precise timing and control over quantum states. Usually, electronic signals are sent into vacuum chambers via wire feedthroughs, and laser light is focused down to a trapped ion's location with external lenses mounted outside viewports on the chamber. These requirements lead to dense and complex setups that may be prone to drift and limit the amount of control that can be achieved.

We have made recent progress toward integrating control technology into the substrate of the ion trap itself. By using a planar trap design, which is compatible with lithographic fabrication, we may implement other well-developed processes in order to enhance the function of the ion trap. In one experiment, we demonstrate an ion trap with integrated, complementary metal-oxide-semiconductor-based high-voltage sources that can be used to control the motional frequency and position of a trapped ion. In another demonstration, we use photonic waveguides and diffractive grating couplers to route light around a chip and focus it onto ions trapped above the surface.

Integrating controls into ion traps has the potential to increase the density of independently controllable ions on a chip in next-generation systems, but there are also many immediate practical benefits. Reducing the number of required feedthroughs allows chambers to be made more compact, which may be useful for ion-based clocks or sensors. We also show that integrated-photonic platforms help to reduce vibration-induced noise seen when using external optics, which may enable portable systems based on trapped-ion quantum information processing.

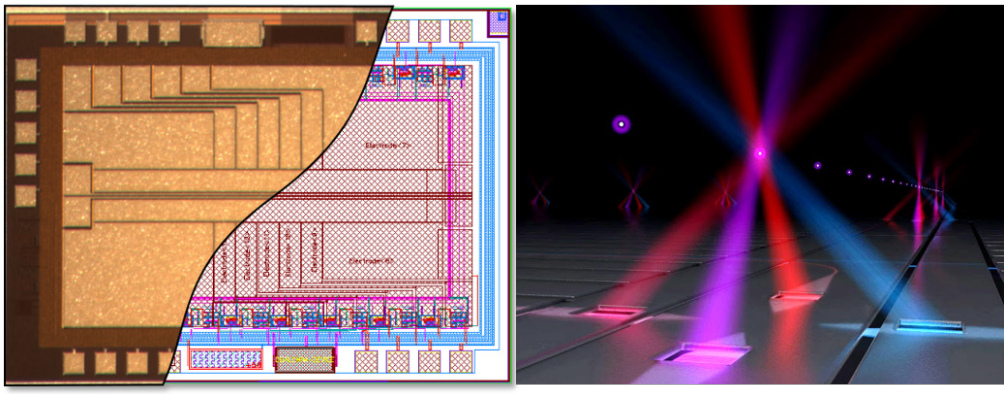

▲ Figure 1: Cutaway view of an ion trap with integrated electronics. The micrograph shows the top metal layer of the integrated circuit, with trap electrodes, and the circuit diagram shows the active voltage sources in the interior layers. [Right] Notional depiction of laser light focusing above an ion trap using integrated photonics. Diffractive grating couplers (beneath square holes in the plane) direct light of multiple wavelengths from integrated waveguides towards ions trapped above the surface.

FURTHER READING

- R. J. Niffenegger, J. Stuart, C. Sorace-Agaskar, D. Kharas, S. Bramhavar, C. D. Bruzewicz, W. Loh, R. T. Maxson, R. McConnell, D. Reens, G. N. West, J.M. Sage, and J. Chiaverini, "Integrated Multi-wavelength Control of an Ion Qubit", *Nature 586*, 538-542 (2020).
- J. Stuart, R. Panock, C. D. Bruzewicz, J.A. Sedlacek, R. McConnell, I. L. Chuang, J. M. Sage, and J. Chiaverini, "Chip-integrated Voltage Sources for Control of Trapped Ions", *Physical Review Applied 11*, 024010 (2019).